PCCP

RSC Publishing

PERSPECTIVE

View Article Online
View Journal | View Issue

Prospects for graphene–nanoparticle-based hybrid sensors

Cite this: *Phys. Chem. Chem. Phys.*, 2013, **15**, 12785

Perry T. Yin,[a] Tae-Hyung Kim,[bc] Jeong-Woo Choi[c] and Ki-Bum Lee*[ab]

Received 5th May 2013,
Accepted 11th June 2013

DOI: 10.1039/c3cp51901e

www.rsc.org/pccp

Graphene is a single-atom thick, two-dimensional sheet of carbon that is characterized by exceptional chemical, electrical, material, optical, and physical properties. As a result, graphene and related materials, such as graphene oxide and reduced graphene oxide, have been brought to the forefront in the field of sensing. Recently, a number of reports have demonstrated that graphene–nanoparticle hybrid structures can act synergistically to offer a number of unique physicochemical properties that are desirable and advantageous for sensing applications. These graphene–nanoparticle hybrid structures are particularly interesting because not only do they display the individual properties of the nanoparticles and of graphene, but they can also exhibit additional synergistic properties thereby enhancing the achievable sensitivity and selectivity using a variety of sensing mechanisms. As such, in this perspective, we will discuss the progress that has been made in the development and application of graphene–nanoparticle hybrid sensors and their future prospects. In particular, we will focus on the preparation of graphene–nanoparticle hybrid structures as well as their application in electronic, electrochemical, and optical sensors.

1. Introduction

The term "graphene" refers to single-atom thick sheets of sp^2 bonded carbon atoms that are arranged in a perfect honeycomb lattice. Since its discovery in 2004,[1] graphene has quickly become an exceedingly hot topic in a number of fields including electronics,[2] energy,[3,4] and sensing.[5–8] Specifically, owing to its structure,

[a] *Department of Biomedical Engineering, Rutgers, The State University of New Jersey, Piscataway, NJ, USA*
[b] *Department of Chemistry and Chemical Biology, Rutgers, The State University of New Jersey, Piscataway, NJ, USA. E-mail: kblee@rci.rutgers.edu; Fax: +1 732-445-5312; Tel: +1 732-445-2081*
[c] *Department of Chemical and Biomolecular Engineering, Sogang University, Seoul, Republic of Korea*

Perry T. Yin

Perry To-tien Yin is pursuing his PhD in Biomedical Engineering at Rutgers, The State University of New Jersey. He received his BS in Biomedical Engineering from Columbia University in 2010 where he concentrated on biomechanics and tissue engineering. His research interests mainly focus on applying multifunctional nanoparticles for the detection and treatment of breast and brain cancer with particular emphasis on the application of magnetic nanoparticles for magnetic hyperthermia. He has published more than 6 peer-reviewed papers in Sci. Rep., Adv. Mater., Angew. Chem., Int. Ed., etc.

Tae-Hyung Kim

Tae-Hyung Kim is working in the Department of Chemistry & Chemical Biology at Rutgers, The State University of New Jersey, as a Postdoctoral Research Associate. He received his PhD from Sogang University, South Korea, under the supervision of Dr Jeong-Woo Choi. His research mainly focuses on the development of cell-based chips that integrate nanotechnology with techniques related to stem cells and cancer cells. He has published more than 20 peer reviewed papers in Biomaterials, Anal. Chem., Nanomedicine: NBM, Biosens. Bioelectron., etc.

graphene is characterized by exceptional biological (*e.g.* biocompatibility), electrical (*e.g.* high carrier mobility and capacity), electrochemical (*e.g.* high electron transfer rate), mechanical (*e.g.* robust and flexible), optical (*e.g.* high opacity, able to quench fluorescence), and structural properties (*e.g.* high surface-to-volume ratio).[9,10] As a result, graphene has a particularly enormous potential for use in sensing applications to detect a wide variety of targets including, but not limited to, biomolecules, chemicals, and even living cells.

Despite its recent discovery, graphene has already demonstrated its superiority to the well-established carbon nanotube in terms of electrocatalytic activity and macroscopic scale conductivity thereby suggesting its potential to excel in other areas as well.[11,12] For electrochemical sensors, graphene is an ideal material due to its large electrochemical potential window ($\sim$2.5 V in 0.1 mM phosphate buffered saline).[13] Recent reports have demonstrated that graphene-based electrochemical sensors have superior performance to carbon nanotubes, due to the presence of more sp^2-like planes and edge defects.[12] Moreover, graphene has an extremely high surface-to-volume ratio, which is theoretically 2600 m^2 g^{-1}, thereby providing a large area for sensing applications.[14] Similarly, for electronic sensors such as field-effect transistors (FETs), graphene offers extremely high carrier mobility, high carrier density, and has low intrinsic noise thereby providing a high signal-to-noise ratio for better detection. On the other hand, graphene is characterized by a zero-bandgap, which makes it very difficult to deplete and hence control the current in the transistor channel.[15,16] However, this can be modulated by altering the gate voltage resulting in the exhibition of ambipolar properties. The zero-bandgap can also be opened by reducing the dimensions of the graphene sheets to the nanoscale[17,18] or by introducing dopants.[19,20] In this way, the sensitivity of graphene FETs is superior to conventional metallic microelectrodes and comparable to silicon nanowire FETs.[21,22] On the other hand, graphene related materials such as graphene oxide (GO) and reduced graphene oxide (rGO) have the unique feature in that they, themselves, are fluorescent and also have the ability to quench the fluorescence of molecules adsorbed onto their surface such as dyes, polymers, or quantum dots.[23] Theoretically, the quenching efficiency of GO or rGO can be as high as 10^3 and as a result, fluorescence quenching can be used for various sensing applications such as for the detection of single-stranded DNA or biomolecules.[24] In particular, such sensors have been reported with detection limits as low as 100 nM and can be fabricated at a very low cost.[25]

Recently, it was reported that the properties of graphene-based sensors could be tuned by incorporating nanoparticles (*e.g.* metallic, oxide, and semiconductor nanoparticles) with graphene sheets to form graphene–nanoparticle hybrid structures.[26] As such, many efforts have since been made to functionalize graphene with different nanoparticles in order to enhance their individual properties and bring additional

Jeong-Woo Choi

Jeong-Woo Choi received his PhD in 1990 at Rutgers, The State University of New Jersey. He worked at the IBM Almaden Research Center and Mitsubishi Electronics Advanced Technology R&D Center as a visiting researcher from 1993 to 1996. He also obtained a D. Eng. from Tokyo Institute of Technology, Japan, in 2003 as well as an MBA degree from the University of Durham, UK. He has been a Professor of the Department of Chemical & Biomolecular Engineering, Sogang University, South Korea, for over 23 years. He is a leading researcher in the field of nanobioelectronics including biomemory, nanoprotein chips, and cell chips. He has published over 306 peer-reviewed papers in Adv. Mater., Biomaterials, Biosens. Bioelectron., etc.

Ki-Bum Lee

Ki-Bum Lee was recently promoted to an Associate Professor with tenure in the Department of Chemistry and Chemical Biology at Rutgers University, where he has been a faculty member since 2008. He received his PhD in Chemistry from Northwestern University (with Chad. A. Mikrin; 2004) and completed his post-doctoral training at The Scripps Research Institute (with Peter G. Schultz; 2007). The primary research interest of Dr Lee's group is to develop and integrate nanotechnologies and chemical functional genomics to modulate signaling pathways in cells (e.g. stem cells and cancer cells) towards specific cell lineages or behaviors. In recognition of his outstanding scientific achievement at Rutgers, Dr Lee has received several awards including NIH Director's New Innovator Awards (2009), the Board of Trustees Research Award for Scholarly Excellence (2013), the Johnson and Johnson Proof-of-Concept Award (2011), the Faculty Research Grant Award (2012), the New Jersey Spinal Cord Research Award (2009), and the Grant Proposal Development Award (2008). Moreover, he is the author of over 30 articles published in Science, Cell Stem Cell, J. Am. Chem. Soc., Angew. Chem., Int. Ed., Nano Letters, ACS Nano, Adv. Mater., Sci. Rep., Lab Chip, Small, and Cancer Res., which are highly cited (>2800).

advantages for sensing applications. For example, graphene–nanoparticle hybrid structures have been applied to areas including electronic and electrochemical sensing, surface enhanced Raman scattering (SERS), and catalysis. These graphene–nanoparticle hybrid structures are particularly interesting for sensing applications because not only do they display the individual properties of graphene and the nanoparticles, but they can also exhibit additional synergistic properties.

In this perspective, we will survey the emerging application of graphene–nanoparticle hybrid structures for biological and chemical sensing. Several excellent reviews on the basic science of graphene and graphene-based sensors have already been published.[10,27] However, given the growing interest in graphene–nanoparticle hybrid structures for sensing applications, a review focusing on graphene–nanoparticle hybrid materials is very appropriate. Emphasis will be placed on the preparation of graphene–nanoparticle hybrid materials and their application to electronic, electrochemical, and optical sensors (*e.g.* SERS and FRET-based sensors). In particular, we aim to provide a comprehensive review that covers the latest and most significant developments in this field and offer insight into future prospects. We hope that this article will inspire interest from various disciplines and highlight an up and coming field wherein graphene–nanoparticle hybrid structures can bring synergistic advantages to a wide variety of sensing applications.

2. Preparation and properties of graphene materials

As mentioned previously, due to the many unique and advantageous properties of graphene and its related materials such as GO or rGO, a significant amount of research has been conducted in order to apply these materials either by themselves, or in combination with other interesting nanomaterials such as nanoparticles. In the following section, we will describe the fabrication methods used to produce graphene, GO, and rGO as well as graphene–nanoparticle structures including graphene–nanoparticle composites and graphene-encapsulated nanoparticles.

2.1 Graphene and graphene oxide

Unlike graphite, graphene is highly conductive (mobility: 2 00 000 $cm^2\ V^{-1}\ s^{-1}$), transparent (transmittance: ~97.7%) and has high mechanical strength (Young's modulus: ~1.0 TPa) resulting in its utility for electronic, electrochemical, and optical sensing.[28,29] In particular, graphene sheets can be obtained using a number of methods including mechanical exfoliation (*e.g.* the Scotch tape method), chemical vapor deposition (CVD) on metal or Si substrates, and the chemical/electrochemical reduction of graphene oxide (Fig. 1).[30] In terms of mass production, the CVD method can be used to fabricate large areas, which have a small number of defects. For example, Hong *et al.* reported that large-area graphene synthesis is possible using a roll to roll production method, which is an application of the CVD method.[31,32] The reduction of graphene oxide has also been demonstrated to be a relatively economical and facile technique

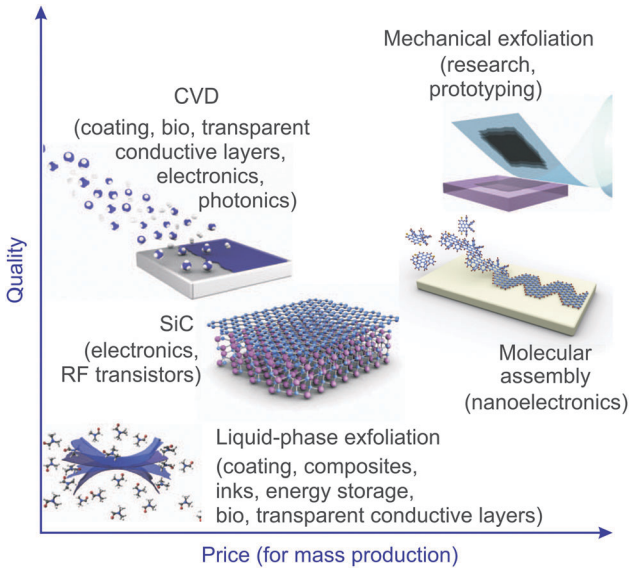

Fig. 1 Methods for the mass-production of graphene. There are several choices depending on the particular application, each with differences in terms of size, quality, and price. Reproduced from ref. 10 with permission from Nature.

for the production of graphene; however, the quality of reduced graphene in terms of electrical conductivity is reported to be lower than that of graphene sheets produced using the CVD method. As such, the reduction method is a better fit for producing small graphene sheets while CVD is more efficient for the mass-production of graphene. Hence, the application for which graphene is being synthesized must first be considered before the proper production method can be chosen (Fig. 1).

GO, a derivative of graphene, has many distinct characteristics that are very different from those of graphene due to the presence of many oxygen containing groups (–C–O–C–, C–O–H,–COOH, *etc.*) that act to inhibit electron transfer. However, it is still mechanically strong, flexible, transparent, and biocompatible owing to its hydrophilic nature. The Brodie, Staudenmaier, and Hummer methods are all very common protocols for the production of GO and involve the oxidation of graphite to obtain hydrophilic groups on the surface. In particular, a combination of potassium chlorate ($KClO_3$) and nitric acid (HNO_3) is used to oxidize graphite in the Brodie and Staudenmaier methods while permanganate ($KMnO_4$) and sulfuric acid (H_2SO_4) are used in the Hummer method.[33,34] After the oxidation process, the resulting product must be exfoliated to obtain one- or multi-layer GO sheets. Specifically, this can be achieved using ultra-sonication.

Finally, rGO can be obtained from GO through chemical or electrochemical reduction, which removes the oxygen-containing branches from the basal planes and edges of the GO sheet.[29] For this purpose, hydrazine, hydroquinone, ascorbic acid, and sodium borohydride are commonly used to remove the hydroxyl groups of GO. Electrochemical tools can also be used to fabricate rGO. Specifically, this can be accomplished using either sulfuric acid or non-acidic solutions such as Na-phosphate-buffered saline (PBS), K-PBS, NaOH, and KCl when the solution is applied to a

constant reduction potential or to sweeping potentials.[35] The rGO that is produced *via* chemical reduction is often referred to as 'crGO' while electrochemically reduced GO can be known as 'erGO'. However, both types of rGOs lack the excellent electrical conductivity of graphene (~ 0.36 S m^{-1}) due to broken π-conjugated structures and the remaining hydroxyl groups but can be advantageous for certain applications.[36] To recover the electrical conductivity, recent studies have demonstrated that the deoxygenation of rGO sheets with sodium borohydride followed by dehydration with sulfuric acid and annealing of carbon bonds with Ar gas under high temperatures (~ 1100 °C) can be an effective method.[37] In particular, according to the author's report, the final rGO product has an electrical conductance of 2.02×10^4 S m^{-1}, which is four orders of magnitude higher than that of GO. On the other hand, recent studies have also demonstrated a laser annealing method as a means to obtain transparent and highly conductive rGO layers. Specifically, it is based on the use of a laser beam for the *in situ*, nonthermal, reduction of GO films. Due to this exposure, there is selective removal of the oxygen species, which takes place in air without the occurrence of ablation. By carefully tuning the laser parameters, the degree of GO reduction can be controlled. The major advantage of this technique is that it is a one-step facile process that can be rapidly carried out at room temperature in air without affecting the integrity of the graphene lattice or the flexibility of the underlying substrate.[38,39]

2.2 Graphene–nanoparticle composites

Graphene–nanoparticle composites can be obtained by anchoring various types of nanoparticles to the surface of graphene, GO, or rGO through both covalent or non-covalent bonding (Fig. 2a and b).[40] In particular, the presence of defects and oxygen functional groups make GO and rGO promising templates for the nucleation and growth of metallic nanostructures including Au,[41] Ag,[42] TiO_2,[43] and even Fe_3O_4 nanoparticles.[44] Since both the metal nanoparticles that are used to decorate the surface of graphene/GO nanosheets and graphene itself have excellent electron transfer properties and are both ideal templates for conjugation chemistry, the combination of these two different materials is proving to be a very powerful strategy for the detection of specific targets. Moreover, the structural characteristics of graphene result in an excellent ability to adsorb specific molecules *via* π–π and electrostatic interactions, which further contributes to the enhancement of electronic, electrochemical, and/or optical signal measurement in terms of selectivity and sensitivity.[29] Even more remarkably, the distinct Raman peaks such as the D, G, and 2D bands that are characteristic of graphene/GO can be used as excellent probes for Raman reporters.[28] For example, based on these characteristics, Li *et al.* have reported that GO conjugated with gold clusters can act as an effective platform to study the uptake of hybrid structures into cells. Moreover, these constructs could be used to reveal the underlying mechanism of uptake based on the use of surface-enhanced Raman spectroscopy (SERS).[45]

Graphene–metal nanoparticle composites are normally fabricated *via* the reduction of metallic salts using well-known chemical agents such as ethylene glycol, sodium citrate, and sodium borohydride.[46,47] More specifically, the negatively-charged functional groups on the surface of GO can induce the nucleation of positively charged metallic salts, resulting in the successful growth of metal nanoparticles on the GO surface. Graphene–metal nanoparticle composites can also be produced using chemical linkers that have a strong affinity for the surface of graphene *via* π–π stacking as previously reported by Zhang *et al.*[48] On the other hand, Deng and co-workers introduced a new nontoxic synthetic method for the fabrication of a graphene composite decorated with various types of nanoparticles (Au, Ag, Pt, Pd, and latex beads) using bovine serum albumin (BSA) that was not only effective for reducing GO to graphene but also for inducing the attachment of nanoparticles onto the graphene surface.[49] Similarly, Wang *et al.* also recently reported an interesting green synthetic method for the production of Ag–GO nanocomposites that utilized glucose as an agent for both reduction and stabilization of Ag nanoparticles, eliminating the need for toxic reduction agents.[50] Besides the chemical reduction methods mentioned above, graphene–nanoparticle composite structures can also be achieved *via* electrochemical techniques. Specifically, Gunasekaran *et al.* reported the electrochemical deposition of graphene–Au/Pd nanoparticle composites onto electrodes by applying a potential of -0.2 V in the presence of metallic salts.[51] Fisher *et al.* also utilized electrochemical tools to fabricate platinum nanoparticle-decorated multilayered graphene nanosheets.[52] According to their report, the density, size, and morphology of the Pt nanoparticles can easily be controlled by adjusting the intensity of the pulse current, indicating that electrochemical techniques can be very useful and advantageous for the fabrication of graphene–nanoparticle composites.

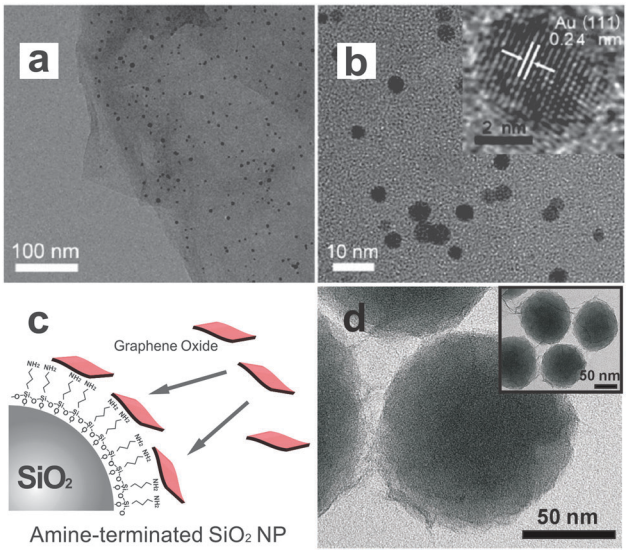

Fig. 2 Transmission Electron Microscopy (TEM) of graphene-encapsulated nanoparticles and graphene–nanoparticle composite structures. (a, b) TEM images of GO–gold nanoparticle sheets at different magnifications. Inset of (b) is a high-resolution TEM of a single gold nanoparticle. Reproduced from ref. 40 with permission from ACS. (c) Negatively charged GO sheets can self-assemble on positive nanoparticles such as SiO_2. (d) TEM of GO-encapsulated SiO_2 nanoparticles. Reproduced from ref. 57 with permission from Wiley.

Lastly, though limited in number, recent reports have demonstrated an interesting 3D graphene-stacked nanostructure that uses nanoparticles as a 'separator'. To this end, Li *et al.* used gold nanoparticle-assembled graphene sheets to fabricate three dimensional structures as confirmed by a gravimetric microcantilever.[53] Similarly, Wang *et al.* also reported the fabrication of 3D nanoparticle-decorated graphene nanostructures using various types of metal nanoparticles (Pd, Pt and Au).[54] Both studies report an enhancement in sensor performance owing to the 3D nanostructures with respect to sensor sensitivity, catalytic activity, and mass transport access when compared to conventional two-dimensional forms.

2.3 Graphene-encapsulated nanoparticles

Owing to the flexible and two-dimensional sheet-like nature of graphene and its derivatives, they can easily be used to wrap or encapsulate spherical nanoparticles (Fig. 2c and d). rGO has been more frequently applied for the encapsulation of nanoparticles because of its hydrophilic characteristics and the ease with which small fractions of rGO can be fabricated. rGO-encapsulated nanoparticles possess a number of advantages when compared to bare nanoparticles including less nanoparticle aggregation as well as the enhancement of electrical, electrochemical, and optical properties.[55] Specifically, owing to the characteristically strong negative charge of rGO the encapsulation of small nanoparticles with rGO results in the suppression of aggregation, which is a major issue in many nanoparticle-based sensing applications. For example, Yang *et al.* have reported that rGO-encapsulated cobalt nanoparticles (Co_3O_4) exhibit a very high reversible capacity (1000 mA h g^{-1}) over 130 cycles, which is superior to normal cobalt oxide nanoparticles that are used for capacitors.[55] Feng and co-workers have also reported graphene-encapsulated TiO_2 nanospheres for efficient photocatalysis owing to their high specific surface area (133 m^2 g^{-1}). The resulting hybrid material had an efficiency of 91% for the decomposition of rhodamine B, which is much higher than the efficiency of normal TiO_2 (65%).[56] We have also reported a method to convert non-conducting silicon oxide nanoparticles into conducting rGO-encapsulated nanoparticles, which could then be used as the 'bridging-material' in a FET-based sensor.[57,58] Finally, Zhang *et al.* recently reported an interesting material, a 'graphene-veiled gold nanostructure'. In this study, they used graphene as a passivation nanosheet to prevent metal–molecule chemical interactions and to control the spatial resolution of molecules in order to achieve sensitive SERS signals from analytes of interest.[59]

Considering the many excellent properties that graphene-encapsulated nanoparticles possess, the process of fabrication is relatively simple. In particular, the most frequently used method for encapsulating nanoparticles with rGO consists of endowing the surface of the nanoparticle with a positive charge, resulting in the strong attachment of rGO *via* electrostatic interaction.[55–58] By controlling the size of cracked rGO, a variety of nanomaterials with varying size including inorganic materials, polymers, metals, and metal oxides can easily be encapsulated by graphene/rGO to enhance their properties as well as to obtain new synergistic effects.

3. Graphene–nanoparticle hybrid materials for sensing applications

In general, sensors are composed of two fundamental elements: a receptor and a transducer. The receptor can consist of any material, either organic or inorganic, that interacts with a target analyte or family of analytes. On the other hand, a transducer is an element that converts the recognition event that occurs between the analyte and the receptor (*e.g.* the binding of an enzyme and its substrate or between an antibody and its target cell or protein) into a measurable signal. This signal can come in many forms including, but not limited to, electrical, electrochemical, and optical. In this section, we will highlight work that has been completed by our group and others on the development of graphene–nanoparticle hybrid sensors for the detection of chemical and biological analytes.

3.1 Electronic sensors

Field-effect transistors (FETs) have received a great deal of attention for use as sensors owing to their ability to provide electronic detection that can be integrated into electronic chips produced by industry today. In fact, a significant amount of work has already demonstrated that graphene-based FET sensors can act as sensitive and selective electronic sensors.[5,6,60] In particular, FET sensors rely on biorecognition events between the analyte of interest and the probe molecules (*e.g.* receptor) at the gate of the FET. Upon recognition or binding of the analyte by the probe, the electric charge distribution changes the conductivity of the channel that exists between the source and drain electrodes. More specifically, this shift is a consequence of a change in the charge carrier density at the biorecognition layer.

Currently, FET sensors that are fabricated using Si nanowires and carbon nanotubes are the most heavily investigated.[61–63] FET sensors that utilize either of these technologies exhibit exceptional performance; however, the use of Si nanowires is expensive. On the other hand, while CNT sensors represent a significantly cheaper option, the reproducibility of these devices in terms of fabrication and electrical properties is considered a significant limiting factor.[64,65] To this end, graphene has a major advantage in FET sensing applications in that graphene has an extremely high surface-to-volume ratio, which should allow it to compete with or surpass CNT and Si nanowire-based FET sensors. More specifically, owing to this high surface-to-volume ratio, any analytes that adsorb onto the graphene surface could potentially alter its electronic properties (*e.g.* the conductivity can be altered when an analyte is adsorbed due to doping or a change in the carrier mobility of graphene).

In the following subsections we will focus on the use of graphene–nanoparticle composites and graphene-encapsulated nanoparticles for FET-based sensing applications.

Graphene–nanoparticle composites. Recent advances have revealed that graphene–nanoparticle hybrid structures can be used in FET sensors to enhance their performance. Demonstrations of graphene–nanoparticle hybrid FET sensors have focused on variations of a single mechanism to enhance performance. Specifically, by conjugating the detection probe (*e.g.* antibody) to the nanoparticle and then using these nanoparticle–probe conjugates to decorate the graphene sheet, one can preserve the superb electrical properties of graphene. For example, Chen *et al.* reported the first graphene–gold nanoparticle hybrid sensor for the detection of proteins.[66] Specifically, thermally-reduced graphene oxide sheets (TRGO) (*e.g.* a few layers with a thickness of 3–6 nm) were decorated with 20 nm gold nanoparticles (AuNPs), which were covalently conjugated to anti-Immunoglobulin G (IgG) antibodies (Fig. 3a). Upon introduction of the target protein (*e.g.* IgG), FET and direct current was measured resulting in a detection limit of approximately 13 pM, which is among the best reported for carbon nanomaterial-based protein sensors including CNTs, graphene, and GO (Fig. 3b). This sensor also showed excellent selectivity when exposed to other protein mismatches such as Immunoglobulin M or horseradish peroxidase (Fig. 3c). In particular, by utilizing such a method where the antibodies are conjugated to the AuNPs, which are then in turn used to decorate the TRGO sheets instead of directly conjugating the antibodies to TRGO, no direct modification was made to the TRGO sheets, preserving its superb electrical properties. According to the authors, binding of the IgGs to anti-IgGs results in local geometric deformations and an increase in the number of scattering centers across the sheet, thereby reducing the mobility of holes and, subsequently, the conductivity of the TRGO sheets.

In 2012, Chen *et al.* also demonstrated that their TRGO–AuNP hybrid FET sensor could be used in chemical detection.[67] Specifically, in this particular study, they functionalized the AuNPs with thioglycolic acid, which allowed for the detection of Hg(II) ions. Again, they demonstrated that their TRGO–AuNP hybrid FET had an excellent performance with a detection limit of 25 nM, which is more sensitive than other reported graphene-based Hg(II) ion sensors and has a response time as fast as a few seconds whereas previous Hg(II) ion sensors were significantly slower.[68–70]

Finally, in another notable work that is along the lines of those described above, Zhang and coworkers reported a Pt nanoparticle (PtNPs)-decorated rGO FET where thiolated probe DNA was attached to the PtNPs *via* a Pt–S bond.[71] This graphene–nanoparticle hybrid FET was then applied for the detection of DNA with a calculated detection limit of 2.4 nM. However, in this case, the PtNPs were directly synthesized onto the rGO sheets by photochemical reduction resulting in a PtNPs–rGO hybrid structure that was used as the channel material of their FET.

Graphene-encapsulated nanoparticles. As a variation of the above-mentioned mechanism, encapsulating nanoparticles with graphene can enhance the surface-to-volume ratio that is available for sensing and capture of the analyte in FET sensors. Recently, our group developed an rGO encapsulated nanoparticle-based FET sensor for the sensitive and selective detection of proteins (Fig. 4a and b).[72] In particular, we sought to detect Human Epidermal growth factor Receptor 2 (HER2) and epidermal growth factor receptor (EGFR), which are both known to be over-expressed in breast cancers.[73] To this end, individual silicon oxide nanoparticles (100 nm diameter) functionalized with 3-aminopropyltriethoxysilane (APTES) were coated with a thin layer of rGO (5 nm thick) owing to the electrostatic interaction that could occur between the negatively charged GO and the positively charged silicon oxide nanoparticles. Arrays of rGO nanoparticles (rGO-NPs) were then patterned to form channels between gold electrodes, which occurred through a self-assembly process upon centrifugation of the device with a solution containing rGO-NPs (Fig. 4c). Finally, the rGO-NPs were functionalized with monoclonal antibodies against HER2 or EGFR. Specifically, this was accomplished using a well-established process where the rGO surface was functionalized with 4-(pyren-1-yl)butanal *via* π–π interactions. Next, the aldehyde groups were coupled to the amine groups of the HER2 or EGFR antibodies through reductive amination and unreacted aldehyde groups were blocked using ethanolamine. In this way, we were able to preserve the electrical properties of the rGO by not conjugating the antibodies directly to the rGO surface. Using this device, we were able to achieve a detection limit as low as 1 pM for HER2 and 100 pM for EGFR (Fig. 4d and f). In addition, we demonstrated

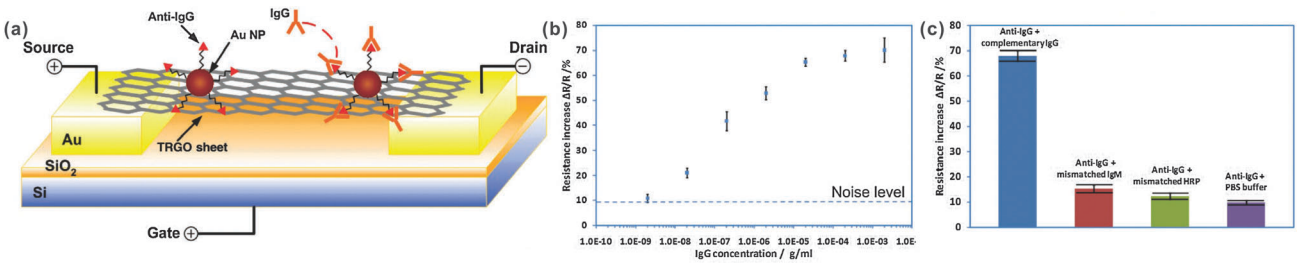

Fig. 3 Protein detection using thermally reduced graphene oxide (TRGO) sheets decorated with gold nanoparticle–antibody conjugates. (a) Schematic of a TRGO FET. Anti-IgG is anchored to the TRGO sheet surface through AuNPs and functions as a specific recognition group for the IgG binding. The electrical detection of protein binding is accomplished by FET and direct current measurements. (b) Sensor sensitivity (relative resistance change, %) *versus* the IgG concentration. The dashed line represents the noise level from the buffer solution. (c) Comparison of the sensor sensitivity in response to complementary IgG, mismatched IgM, mismatched HRP, and PBS buffer. Reproduced from ref. 66 with permission from Wiley.

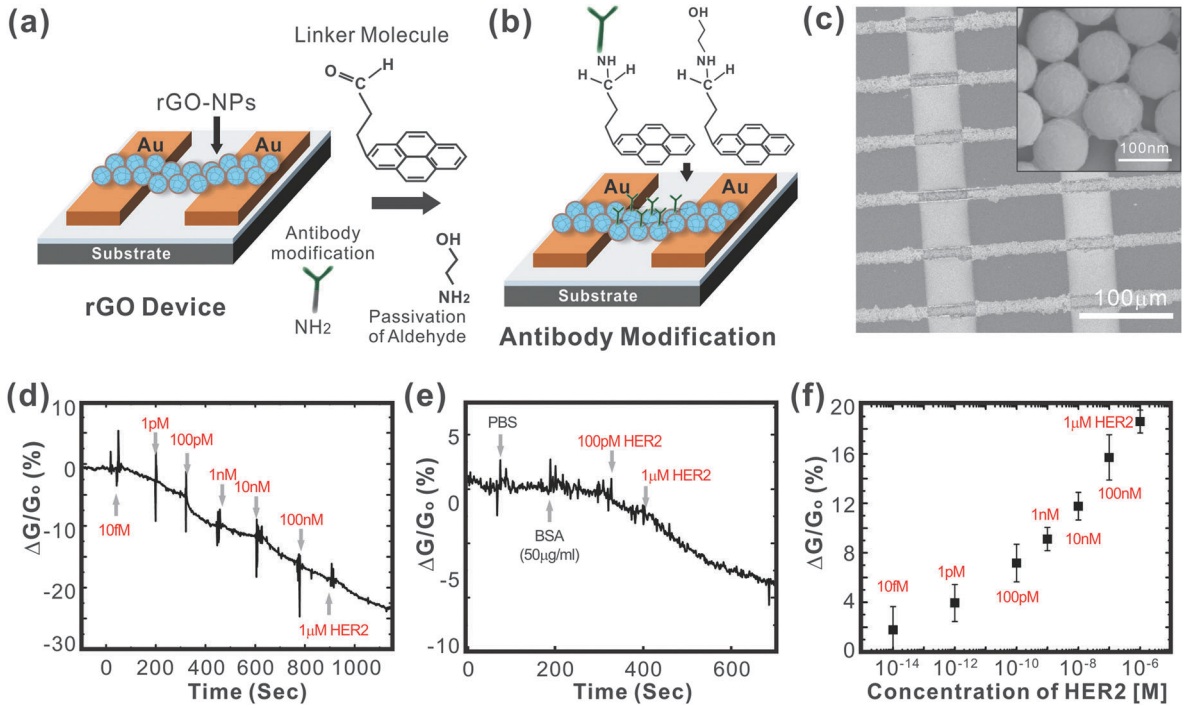

Fig. 4 Graphene-encapsulated nanoparticle-based biosensor. (a) Preparation of the rGO-NP device. (b) Surface functionalization of rGO for immobilizing the antibody. (c) SEM image of biosensor consisting of an rGO-NP array with gold electrodes. (d) Sensitivity of the biosensor (relative conductance change, %) in response to the concentration of HER2. (e) Selectivity of the biosensor in response to PBS, BSA, and HER2. (f) Sensor sensitivity (relative conductance change, %) as a function of the HER2 concentration. Reproduced from ref. 57 with permission from Wiley.

the highly selective nature of our biosensor in the presence of other proteins such as BSA (Fig. 4e).

3.2 Electrochemical sensors

Electrochemical sensors are the largest group of chemical sensors and are highly sensitive to electroactive molecules. A typical electrochemical sensor consists of a sensing (or working) electrode, and a counter electrode, which are separated by a layer of electrolytes. The amount of analyte that is either reduced or oxidized at the sensing electrode would then correlate with the concentration of analyte that is present. For this purpose, graphene is an ideal material as it is an excellent conductor of electrical charge.[74] Moreover, owing to its high surface area, graphene can facilitate the formation of large numbers of defects and thus electroactive sites, owing to the heterogeneous electron transfer that can occur between graphene and the analyte that is being oxidized or reduced.[75] The electrochemical behaviour of graphene is excellent and comparable to other carbon-based materials including carbon nanotubes and graphite. Recent reports have even demonstrated that graphene-based electrochemical sensors have superior performance than carbon nanotubes due to the presence of more sp^2-like planes and edge defects on the surface of graphene.[76]

While graphene exhibits great promise, graphene–nanoparticle hybrid structures have recently gained increasing attention because of their application in electrochemical sensing. In particular, various types of nanoparticles, including metal nanoparticles such as Au and Pt, oxide nanoparticles, and semiconductor nanoparticles are traditional nanomaterials that are widely used for electrochemical sensing applications.[77] These nanoparticles can have different roles in the electrochemical sensing platform; for example, they can function to: (i) immobilize biomolecules,[78] (ii) catalyze electrochemical reactions,[79] or (iii) act as a reactant.[80] As such, by incorporating graphene–nanoparticle hybrid structures, one can impart unique and advantageous properties to electrochemical sensing applications that exhibit the advantages of the individual nanoparticles and graphene as well as synergistic properties of the hybrid material. For example, graphene sheets that are decorated with nanoparticles can help overcome the poor utilization coefficient of aggregated nanoparticles.[81] In certain cases, by decorating graphene with nanoparticles, one can also efficiently improve the electron transfer that occurs between the analyte and the electrode.[82] Finally, similar to what was observed in graphene–nanoparticle hybrid FET sensors, graphene–nanoparticle hybrid structures can facilitate the immobilization of biomolecules to the graphene sheets. Therefore, instead of having to directly immobilize biomolecules to graphene, which itself is a non-trivial matter, the biomolecules can be immobilized on the nanoparticle and then be used to decorate the graphene sheets.

In the following subsections, we will focus on graphene–nanoparticle hybrid structures for the immobilization of biomolecules and the catalysis of electrochemical reactions.

Immobilization of biomolecules. Due to their large specific surface area, graphene–nanoparticle hybrid structures are

advantageous for the immobilization of biomolecules. Moreover, the excellent electrical properties of graphene significantly improve the electronic and ionic transport capacity of the electrochemical sensor. For example, Shan *et al.* gave the first report of an electrochemical biosensor based on a graphene–AuNP nanocomposite for the detection of glucose.[83] Specifically, they demonstrated a novel biosensor where glucose oxidase was immobilized in thin films consisting of a graphene–AuNP–chitosan nanocomposite on a gold electrode (Fig. 5A and B). Chitosan has excellent biocompatibility and film-forming ability and, as such, is an ideal candidate for the immobilization of bioactive molecules onto electrodes.[84,85] The resulting composite film had a detection limit of 180 μM of glucose (Fig. 5C). Moreover, the sensor exhibited good reproducibility and an amperometric response to glucose with a linear range from 2 to 14 mM (Fig. 5D). Shan *et al.* explained this result as a synergistic effect of the graphene–AuNP hybrid structure. Specifically, the presence of graphene in the nanocomposite film improves the electronic and ionic transport capacity, resulting in a considerable enhancement of the electrocatalytic activity toward hydrogen peroxide when compared to AuNPs alone.[86]

Another enzymatic electrochemical sensor utilizing hybrid structures for the detection of glucose was reported by Gunasekaran and co-workers.[51] In particular, a green, simple, fast, and controllable approach was developed where a novel nanocomposite consisting of electrochemically reduced graphene oxide (ERGO) and gold–palladium (1 : 1) nanoparticles (AuPdNPs) was synthesized in the absence of reducing agents. Bimetallic nanoparticles are interesting, especially for electrocatalysis, owing to their ability to offer synergistic effects that enhance electrocatalytic activity, improve biocompatibility, promote electron transfer, and are more poison resistant.[87–89] In particular, Pd is one of the most frequently used electrocatalysts of oxygen reduction reactions and the introduction of Au into the NPs offers many appealing properties such as biocompatibility and provides an excellent surface for biofunctionalization with biomolecules that contain primary amine groups.[90] Glucose oxidase was then immobilized for use as a model enzyme to detect the O_2 consumption that occurs during the enzymatic reaction of GOx. The resulting ERGO–AuPdNP nanocomposite-based electrochemical sensor exhibited excellent biocompatibility and had a detection limit of 6.9 μM, a linear range up to 3.5 mM, and a sensitivity of 266.6 μA mM^{-1} cm^{-2}.

Catalysis of electrochemical reactions. Metal nanoparticles have excellent catalytic properties. The introduction of metal nanoparticles into electrochemical sensors can decrease overpotentials of many electrochemical reactions. To this end, graphene–nanoparticle hybrid structures may have synergistic effects that enhance the overall performance of such sensors. Chen and co-workers have demonstrated that graphene–copper nanoparticle[91] and graphene–nickel nanoparticle[92] hybrid structures can enhance the electrochemical sensing of carbohydrates when compared to nanoparticle systems alone. Again, this is due to the excellent electrical conductance of graphene. In these studies, copper and nickel were chosen based on their wide usage in amperometric detection of carbohydrates and

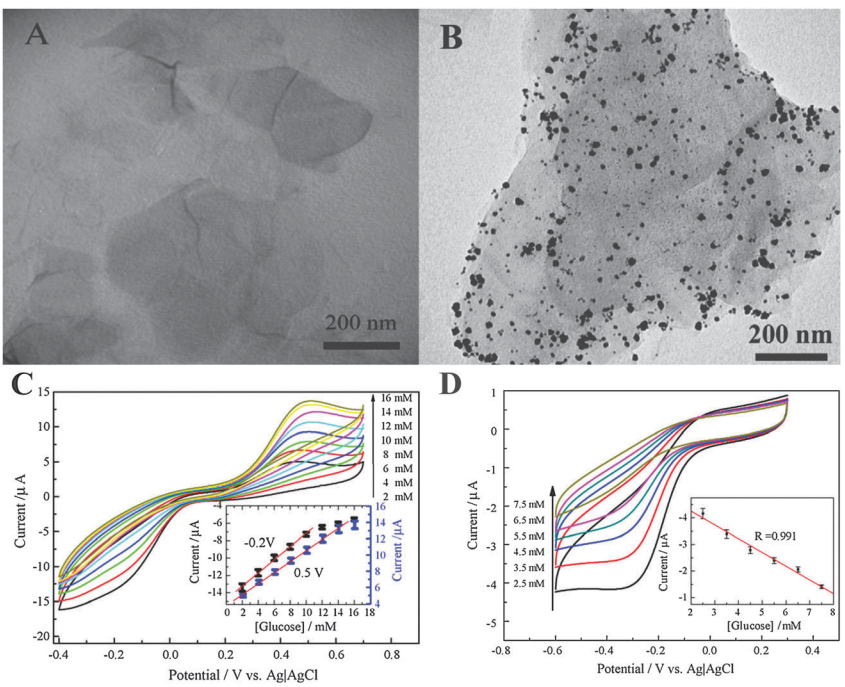

Fig. 5 Graphene–AuNPs–chitosan nanocomposite films for glucose sensing. TEM images of (A) PVP-protected graphene, and (B) AuNPs-decorated graphene. (C) Cyclic voltammetric (CV) measurements of a graphene–AuNPs–chitosan-modified electrode in O_2-saturated phosphate buffer containing various concentrations of glucose: 2, 4, 6, 8, 10, 12, 14, and 16 mM from bottom to top. The inset is the calibration curve corresponding to amperometric responses at −0.2 and −0.5 V. (D) CV measurement in real blood samples and PBS solutions containing 2.5, 3.5, 4.5, 5.5, 6.5, and 7.5 mM glucose from bottom to top. Reproduced from ref. 83 with permission from Elsevier.

their strong electrocatalytic activity with regard to the oxidation of carbohydrates in alkaline solutions, respectively. For example, CuO[93] and NiO[94] nanorod bundles have both been used previously in the direct amperometric detection of carbohydrates and have exhibited strong electrocatalytic activity toward the oxidation of carbohydrates. As such, the authors hypothesized that owing to the excellent properties of graphene, graphene–nanoparticle hybrid structures would enhance the electrochemical sensing of carbohydrates. Specifically, in the case of the graphene–copper nanoparticle hybrid sensor, the hybrid structures were prepared by reducing a mixture containing GO nanosheets and copper(II) ions resulting in the formation of copper particles directly on the surface of graphene.[91] The hybrid material was then packed into fused silica capillaries to form microdisc electrodes. To demonstrate its performance, the graphene–copper nanoparticle composite packed electrode was coupled with a CE system as an end-column amperometric detector for the separation of carbohydrates such as fructose, glucose, lactose, mannitol, and sucrose. The novel detection electrodes were able to separate and detect a mixture of the five carbohydrates. In particular, the sensitivity and detection limit of the sensor was determined to be between 45.61 nA mM^{-1} to 85.96 nA mM^{-1} and 0.87 μM and 1.64 μM, respectively. For comparison purposes, the sensitivity of the sensor for glucose was found to be 63.16 nA mM^{-1} and its detection limit for glucose was 1.19 μM. On the other hand, for the graphene–nickel hybrid sensor (Fig. 6A and B), the graphene–NiNP hybrid was prepared using a one-step far infrared (IR)-assisted reduction of GO and nickel(II) ions in a hydrazine-containing solution.[92] The graphene–nanoparticle hybrid structures were then loaded onto the surface of a magnetic electrode and used to detect a number of carbohydrates including glucose, fructose, lactose, mannose, and sucrose. In comparison to the graphene–CuNP hybrid, the graphene–NiNP hybrid was much easier to load onto the magnetic electrode owing to the ferromagnetic properties of nickel and can be easily fabricated at a low cost. The authors also observed that the graphene–NiNP hybrid sensor had superior performance compared to the graphene–CuNP hybrid sensor. In particular, this sensor exhibited good linearity from 0.001 to 1 mM and a sensitivity of 42.15 nA mM^{-1} (Fig. 6C). Moreover, the detection limit was estimated to be 474 nM and the sensor exhibited good reproducibility (relative standard deviation of 4.3% over 9 measurements). The nickel based hybrid sensor was superior to the copper based one owing to the fact that nickel exhibits a much stronger electrocatalytic activity toward the oxidation of carbohydrates in alkaline solutions.[92] However, in both cases, the presence of graphene greatly enhanced the strength of the electrochemical signal when compared to either nanoparticle (*e.g.* copper or nickel) alone due to the high surface area and excellent electrical properties of graphene.

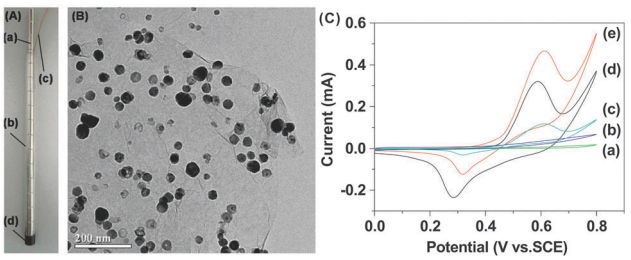

Fig. 6 Magnetic loading of graphene–nickel nanoparticle hybrid for carbohydrate sensing. (A) Photograph of a magnetic electrode: (a) magnet; (b) glass tube; (c) copper wire; (d) graphite–epoxy composite. (B) TEM image of graphene–NiNP hybrid. (C) Cyclic voltammograms of the magnetic electrode before (a), and after being modified by graphene (b), NiNPs (c), graphene–NiNP hybrid (d and e) in 0.1 M NaOH solution containing 0 (d), and 5 mM (a–c and e) glucose at a scan rate of 50 mV s^{-1}. Reproduced from ref. 92 with permission from Elsevier.

The concept of utilizing graphene–nanoparticle hybrid structures for the catalysis of electrochemical reactions has also been extended to the detection of hydrogen peroxide in cells. Jiang and co-workers have recently fabricated an electrochemical sensor that integrates graphene with gold nanoparticles and poly(toluidine blue O) (PTBO) films.[95] The rationale behind this choice is that AuNPs are known to possess excellent catalytic ability for H_2O_2 and can improve the electron transfer between the analyte and the electrode.[96] On the other hand, PTBO provides an ideal matrix to enclose the AuNP–graphene hybrid structures. Specifically, a layer-by-layer approach was used to deposit AuNPs (80 nm) and PTBO film onto RGO. The resulting sensor was characterized by a H_2O_2 sensitivity of 24.52 μA mM^{-1} cm^{-2} and the limit of detection was 0.2 μM. To detect H_2O_2 in living cells, the cells were separated from culture medium and resuspended in deoxygenated PBS. H_2O_2 generation was then stimulated by adding ascorbic acid resulting in the efflux of H_2O_2 from cells, which was detected and quantified by the sensor. In particular, H_2O_2 levels were determined for K562 (human leukemia), PC12 (rat adrenal medulla pheochromocytoma), HepG2 (human hepatocarcinoma), L02 (human embryo liver), and RSC (rat synovial) cells. The results indicate that a higher efflux of H_2O_2 was observed in tumor cells *versus* normal cells. This suggests that there is a decline in enzymatic ROS-scavenging mechanisms in tumor cells as ascorbic acid should induce equal production and distribution of H_2O_2 in tumor and normal cells.

3.3 Optical sensors

In addition to its excellent electronic and electrochemical properties, graphene possesses a number of advantageous optoelectronic properties. Specifically, deoxidation of GO results in the formation of a material that is electrically conductive and optically transparent. Moreover, GO has the unique property in that not only is it fluorescent over a broad range of wavelengths, it can also quench fluorescent molecules such as dyes and quantum dots. As such, by utilizing graphene–nanoparticle hybrid structures, one can impart unique and synergistic properties that can be used for sensing applications. In the following section, we will describe the use of graphene–nanoparticle hybrid materials for optical sensing. In particular, we will focus on Förster or fluorescence resonance energy (FRET) and SERS-based sensors.

FRET-based sensors. FRET is a type of fluorescence phenomenon that involves the sequential excitation and emission of two fluorophores that neighbour each other.[97] Specifically, the

first fluorophore, which is denoted as the 'donor', is initially excited by an external optical source. Excitation of the donor results in a transfer of energy to the neighbouring fluorophore, which is termed the 'acceptor.' This leads to the emission of fluorescence at the acceptor's characteristic wavelength but can also induce quenching of the donor fluorophore. Due to the fact that the intensity of FRET depends strongly on the distance between the two fluorophores and their relative orientation as donors and acceptors, FRET can be used as an excellent biosensing technique that is superior to other optical detection methods in terms of their selectivity and sensitivity.[97,98] Interestingly, graphene and GO were recently found to be super-quenching materials for fluorescence dyes and follow the nano-metal surface energy transfer (NSET) mechanism, which is similar to that of gold nanoparticles. Hence, this strong quenching ability can also contribute to the development of ultra-sensitive sensors by combining graphene materials with other fluorescent nanomaterials.

For example, Ju *et al.* reported a FRET-based biosensor that utilizes small fluorescent nanoparticles known as quantum dots (QDs) and a molecular beacon (MB) to detect specific target ssDNA and thrombin. The LOD (limit of detection) of this system was 0.5 nM and 50 nM for thrombin and ssDNA, respectively, which is highly sensitive and selective when compared to the other fluorescence or FRET-based methods.[99] Wu *et al.* also reported a novel type of GO-based biosensor for monitoring lead(II) using a GO–QDs–aptamer complex.[100] Specifically, these complexes were capable of changing their structural conformation from one dimension to a G-quadruplex–Pb^{2+} complex, leading to the detachment of the QD–aptamer complex from the surface of GO. This detachment then allowed for monitoring using fluorescence microscopy.

Besides the above examples, researchers have tried to combine GO with noble metal nanoparticles to induce a double-quenching effect that would lead to an increase in the achievable signal-to-noise ratio, which is critical for enhancing sensitivity. For example, Qu *et al.* reported a DNA–silver nanocluster–GO nanohybrid material, which could effectively detect multiple nucleic acid targets with a high sensitivity (LOD: 1 nM) and selectivity.[101] Chen and co-workers also reported a similar detection platform that utilized gold nanoparticle-functionalized graphene for the detection of lead ions (Fig. 7). This sensor was found to function in the concentration range of 50–1000 nM and had a LOD of 10 nM.[102] Remarkably, a variety of sensors can be developed based on FRET by utilizing GO–nanoparticle hybrids together with nucleotide-based materials such as RNAs, DNAs, or aptamers due to π–π interaction. This interaction is not only useful for attaching ssDNA/RNA but can also be useful for releasing it from the surface of GO, which ultimately contributes to the enhancement of sensitivity and selectivity.

SERS-based sensors. It has become a common practice to use nanoparticles/nanostructures composed of noble metals (*e.g.* Cu, Ag or Au) to enhance Raman signals owing to electromagnetic enhancement. Interestingly, recent studies have found that graphene or GO also have the ability to increase

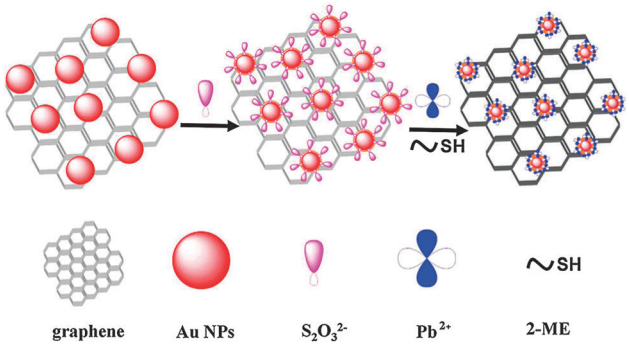

Fig. 7 Fluorescence detection of lead ions based on graphene–gold nanoparticle composite structures. Schematic representation of the sensing mechanism for the detection of Pb^{2+} ions based on accelerated leaching of gold nanoparticles on the surface of graphene. Reproduced from ref. 102 with permission from ACS.

Raman signals *via* a chemical enhancement mechanism, which is independent from that of noble metal nanoparticles.[103] Hence, it can be expected that the combination of graphene and metal nanoparticles would act synergistically to further enhance SERS than by either graphene or metal nanoparticles alone (*e.g.* dual-enhancement of Raman signals *via* chemical and electromagnetic enhancement).[59] Using this strategy, graphene–nanoparticle hybrid materials have been developed to successfully detect a variety of biomolecules and toxic materials. For example, Wang *et al.* developed an Ag–GO nanohybrid structure that can function as a Raman-enhancing material to detect folic acid in water. In particular, this sensor exhibited a linear response between 9 nM–180 nM even when mixed with serum proteins.[104] Interestingly, the authors reported that the common Raman agent (p-ATP), which was used as a control, was strongly enhanced on the normal Ag nanoparticles while the Raman signals of folic acid were much higher on Ag–GO nanohybrid structures than on normal Ag nanoparticles due to the presence of strong electrostatic interaction. The Ag–GO nanostructures were further applied to monitor four varieties of prohibited colorants in food, as well as to detect H_2O_2–glucose without the need for glucose-oxidase (GOD) where a LOD of 100 μM and 7 μM, respectively, was achieved.[105,106] Similarly, Long *et al.* recently reported a disposable biosensor composed of an Ag–GO nanocomposite on a screen-printed electrode that was capable of monitoring different polar antibiotics *in situ* with a LOD of 1 nM using SERS (Fig. 8).[107] Furthermore, Chen and co-workers also reported a SERS-based sensor that was composed of *p*-aminothiophenol-deposited Ag–GO hybrid nanostructure, which was very sensitive for the detection of 2,4,6-trinitrotoluene (TNT).[108] The experimental LOD of the fabricated sensor was 10 pM while the theoretical LOD was found to be as low as 100 aM, indicating that GO–metal nanoparticle hybrid materials are very promising for the development of rapid, sensitive, and selective SERS-based sensors.

Besides the SERS enhancing characteristics of GO–metal composite structures, there are many additional interesting applications of GO nanocomposites especially for cellular

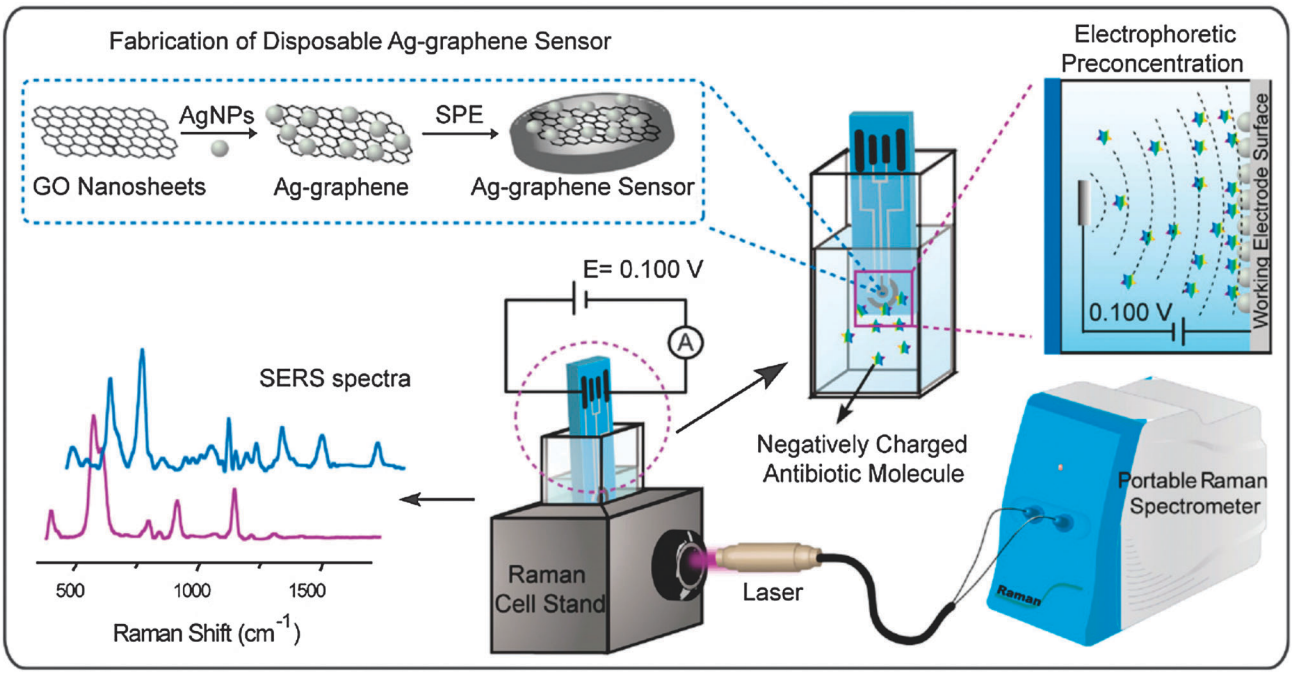

Fig. 8 Schematic representation of a disposable Ag–graphene sensor for the detection of polar antibiotics in water. The magnification insets show the fabrication of Ag–graphene sensors and the electrophoretic preconcentration process of polar antibiotics. The distribution of antibiotics molecules is sketched for the case of a negatively charged analyte. At a given potential, most of the negatively charged antibiotics are concentrated onto the positively charged printed electrode, due to the generated electric field between the working electrode and the counter electrode. In SERS experiments, the laser comes vertically from the side view of the spectroelectrochemical cell and is focused on the Ag–graphene sensor. Reproduced from ref. 102 with permission from Elsevier.

applications. Guo *et al.* recently reported an intracellularly produced gold nanoparticle modified by poly(vinylpyrrolidone) (PVP)-functionalized graphene oxide (GO) which was named as PVP/GO/IGAuNs.[109] The distribution of PVP/GO/IGAuNs in cells then allowed for the sensitive monitoring of intracellular chemical compositions including the cytoplasm, nucleoplasm, and even the nucleus using SERS. Moreover, Yang *et al.* also reported GO–Ag nanoparticles, which enabled very rapid cancer cell probing and imaging with a detection time of 0.06 s per pixel.[110] In this particular case, the authors demonstrated a possible application by conjugating folic acid on the surface of GO, which enabled the sensitive monitoring of the reactions between folic acid and folate receptors.

4. Conclusions and future prospects

The immense potential of graphene to be applied to various applications spanning multiple fields has culminated in the awarding of the 2010 Nobel Prize in Physics to Novoselov and Geim. Within the field of chemical and biological sensors, graphene has already received a significant amount of attention. More recently, graphene–nanoparticle hybrid materials are of particular interest owing to the unique and advantageous properties of each separate material and their synergism for use in sensing applications. In this perspective, we have reviewed graphene–nanoparticle hybrid sensors that are based on electronic, electrochemical, and optical sensing mechanisms. In all cases, graphene–nanoparticle hybrid sensors offer sensitive and selective sensing that is comparable or better than gold standards including other carbon-based nanomaterials while bringing additional advantages (Table 1).

In terms of their future prospects, graphene–nanoparticle hybrids can not only push the limits of achievable sensitivity and selectivity but can also offer a number of multifunctionalities. For example, outside of sensing, graphene–nanoparticle hybrid materials are being developed for applications such as catalysis, photovoltaic devices, supercapacitors, and can also be used in drug delivery or as clinical imaging agents. On the other hand, in the field of chemical and biological sensing, we can expect that graphene–nanoparticle hybrid structures will continue to improve electronic, electrochemical, and optical sensing techniques for the detection of not only biological and chemical molecules but even entire living cells (*e.g.* stem cell differentiation). Graphene–nanoparticle hybrid structures will also offer the ability to develop novel sensing mechanisms. For example, our group has recently developed a label-free polypeptide-based biosensor for enzyme detection using graphene–AuNP composites (Fig. 9a).[58] In particular, in this platform, graphene is first deposited between Au electrodes (Fig. 9c). A layer of functional polypeptide linker followed by AuNPs is then assembled on the graphene layer (Fig. 9b). In this way, enzymatic degradation of the functional polypeptide linker by the enzyme of interest results in release of the AuNP and a measurable shift in electrical hysteresis. Using such a method, we achieved the sensitive (LOD 1 μM) and selective detection of carboxypeptidase B, a predictor for severe acute

Table 1 Summary of the different detection mechanisms discussed

Type	Typical NPs	LOD	Advantages	Ref.
FET	Au, Pt, SiO_2	~1 pM	1. Enhanced surface area for detection 2. Preserve the electrical properties of graphene by conjugating the probe on the nanoparticle	66, 67, 71, 72
Electrochemical	Au, AuPd, Cu, Ni	~100 nM	1. Immobilization of biomolecules 2. Catalyze electrochemical reactions 3. Act as a reactant	51, 83, 91, 92, 95
FRET	QDs, Au, Ag	~10 nM	1. GO is superquenching, which can result in double-quenching (*e.g.* with Au or Ag)	99–102
SERS	Au	~10 pM	1. Dual enhancement of Raman signals *via* chemical and electromagnetic enhancement	104–108

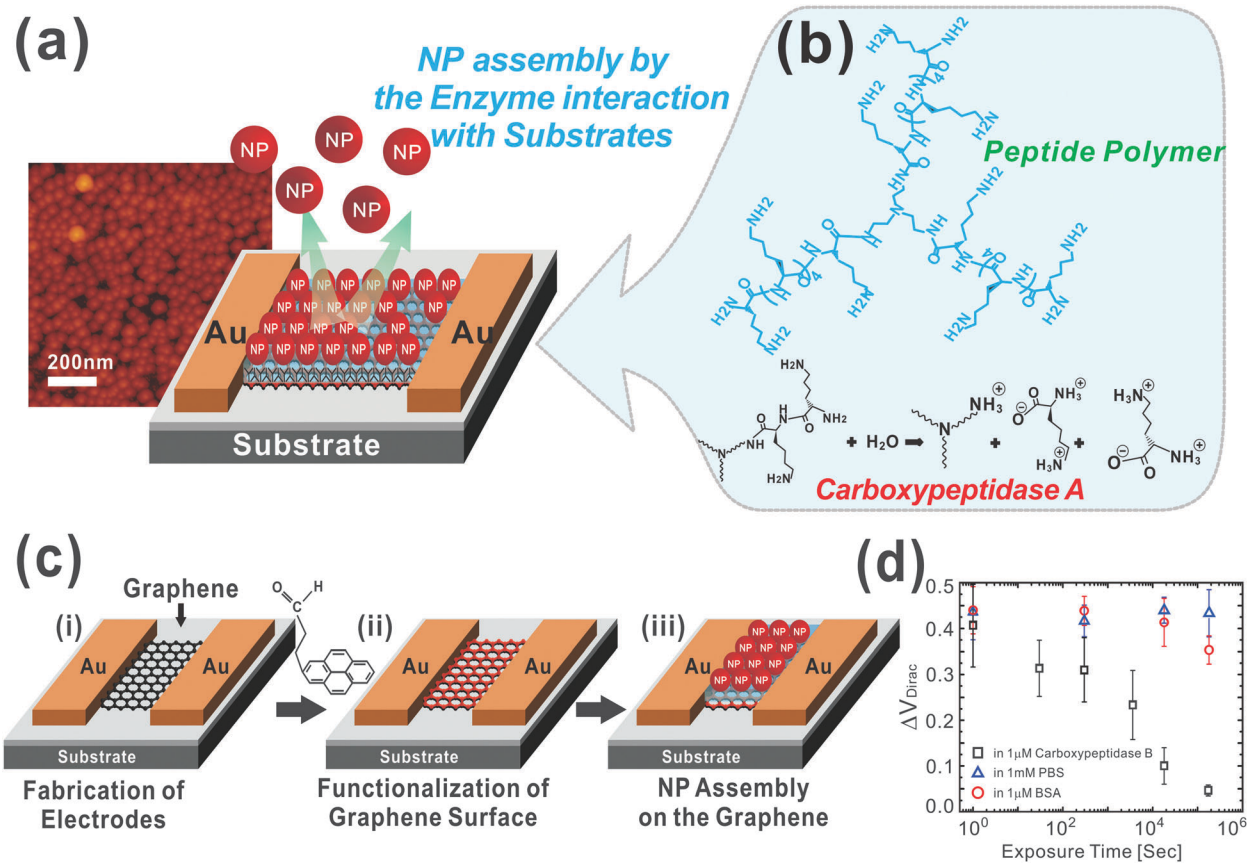

Fig. 9 Hysteresis-based enzyme detection using a graphene–nanoparticle hybrid sensor. (a) Graphene–nanoparticle hybrid devices for enzyme sensing. (b) Chemical structure of the functional polypeptide linker molecule. (c) Fabrication process of the hybrid biosensor. Fabrication of the graphene channel between the Au electrodes (i). Functionalization of the graphene surface with hydrophilic molecules (ii). Assembly of the functional peptide linker molecules and AuNPs on the polypeptide layer (iii). (d) Change in V_{Dirac} under various periods of exposure to a 1 μM solution of carboxypeptidase B in PBS, 1 mM PBS solution and 1 mM solution of BSA in PBS. Reproduced from ref. 58 with permission from Wiley.

pancreatitis (Fig. 9d). In terms of its mechanism, the AuNPs assembled on the graphene surface using a functional polypeptide linker have the ability to store charge resulting in a measurable hysteresis upon their release from the device surface.

In conclusion, while promising, the field of graphene–nanoparticle hybrid sensors is still in its infancy and a number of challenging issues remain to be addressed. For example, with regard to the fabrication of graphene–nanoparticle composites the key hurdle lies in the achievement of reproducible structures wherein the nanoparticles are dispersed uniformly on the graphene sheets. In the case of graphene-encapsulated nanoparticles, a similar obstacle is faced wherein thin carbon shells should ideally be formed uniformly on all nanoparticles. By attaining this high level of uniformity and reproducibility in both graphene–nanoparticle composites as well as graphene-encapsulated nanoparticles, we will be able to maximize the electrical properties of the devices and as such, maximize their sensitivity and selectivity. Fortunately, given its great potential, we believe advances in this field will be made rapidly. Moreover, maturation of this technology will allow for the high-quality and large-scale fabrication of graphene–nanoparticle

hybrid sensors while minimizing costs leading to its commercialization.

Notes and references

1 K. S. Novoselov, A. K. Geim, S. V. Morozov, D. Jiang, Y. Zhang, S. V. Dubonos, I. V. Grigorieva and A. A. Firsov, *Science*, 2004, **306**, 666–669.
2 J. Wu, W. Pisula and K. Müllen, *Chem. Rev.*, 2007, **107**, 718–747.
3 J. Zhang, F. Zhao, Z. Zhang, N. Chen and L. Qu, *Nanoscale*, 2013, **5**, 3112–3126.
4 S. Han, D. Wu, S. Li, F. Zhang and X. Feng, *Small*, 2013, **9**, 1173–1187.
5 R. Stine, S. P. Mulvaney, J. T. Robinson, C. R. Tamanaha and P. E. Sheehan, *Anal. Chem.*, 2013, **85**, 509–521.
6 Y. Liu, X. Dong and P. Chen, *Chem. Soc. Rev.*, 2012, **41**, 2283–2307.
7 D. A. Brownson, D. K. Kampouris and C. E. Banks, *Chem. Soc. Rev.*, 2012, **41**, 6944–6976.
8 K. P. Loh, Q. Bao, G. Eda and M. Chhowalla, *Nat. Chem.*, 2010, **2**, 1015–1024.
9 M. J. Allen, V. C. Tung and R. B. Kaner, *Chem. Rev.*, 2010, **110**, 132–145.
10 K. S. Novoselov, V. I. Fal'ko, L. Colombo, P. R. Gellert, M. G. Schwab and K. Kim, *Nature*, 2012, **490**, 192–200.
11 Y. Wang, Y. M. Li, L. H. Tang, J. Lu and J. H. Li, *Electrochem. Commun.*, 2009, **11**, 889–892.
12 S. Alwarappan, A. Erdem, C. Liu and C. Z. Li, *J. Phys. Chem. C*, 2009, **113**, 8853–8857.
13 M. Zhou, Y. M. Zhai and S. J. Dong, *Anal. Chem.*, 2009, **81**, 5603–5613.
14 Z. Y. Zhong, W. Wu, D. Wang, D. Wang, J. L. Shan, Y. Qing and Z. M. Zhang, *Biosens. Bioelectron.*, 2010, **25**, 2379–2383.
15 T. J. Echtermeyer, M. C. Lemme, M. Baus, B. N. Szafranek, A. K. Geim and H. Kurz, *IEEE Electron Device Lett.*, 2008, **29**, 952–954.
16 G. Fiori and G. Iannaccone, *IEEE Electron Device Lett.*, 2009, **30**, 1096–1098.
17 V. Barone, O. Hod and G. E. Scuseria, *Nano Lett.*, 2006, **6**, 2748–2754.
18 M. Han, B. Ozyilmaz, Y. Zhang, P. Jarillo-Herero and P. Kim, *Phys. Status Solidi B*, 2007, **244**, 4134–4137.
19 X. C. Dong, D. L. Fu, W. J. Fang, Y. M. Shi, P. Chen and L. J. Li, *Small*, 2009, **5**, 1422–1426.
20 D. C. Wei, Y. Q. Liu, Y. Wang, H. L. Zhang, L. P. Huang and G. Yu, *Nano Lett.*, 2009, **9**, 1752–1758.
21 T. Cohen-Karni, Q. Qing, Q. Li, Y. Fang and C. M. Lieber, *Nano Lett.*, 2010, **10**, 1098–1102.
22 Y. M. Lin, C. Dimitrakopoulos, K. A. Jenkins, D. B. Farmer, H. Y. Chiu, A. Grill and P. Avouris, *Science*, 2010, **327**, 662.
23 K. P. Loh, Q. L. Bao, G. Eda and M. Chhowalla, *Nat. Chem.*, 2010, **2**, 1015–1024.
24 L. M. Xie, X. Ling, Y. Fang, J. Zhang and Z. F. Liu, *J. Am. Chem. Soc.*, 2009, **131**, 9890–9891.
25 C. H. Lu, H. H. Yang, C. L. Zhu, X. Chen and G. N. Chen, *Angew. Chem., Int. Ed.*, 2009, **48**, 4785–4787.
26 S. Bai and X. Shen, *RSC Adv.*, 2012, **2**, 64–98.
27 A. K. Geim and K. S. Novoselov, *Nat. Mater.*, 2007, **6**, 183–191.
28 C. N. R. Rao, A. K. Sood, K. S. Subrahmanyam and A. Govindaraj, *Angew. Chem., Int. Ed.*, 2009, **48**, 7752–7777.
29 Y. W. Zhu, S. Murali, W. W. Cai, X. S. Li, J. W. Suk, J. R. Potts and R. S. Ruoff, *Adv. Mater.*, 2010, **22**, 3906–3924.
30 X. S. Li, W. W. Cai, J. H. An, S. Kim, J. Nah, D. X. Yang, R. Piner, A. Velamakanni, I. Jung, E. Tutuc, S. K. Banerjee, L. Colombo and R. S. Ruoff, *Science*, 2009, **324**, 1312–1314.
31 S. H. Ahn and L. J. Guo, *Adv. Mater.*, 2008, **20**, 2044–2049.
32 S. Bae, H. Kim, Y. Lee, X. F. Xu, J. S. Park, Y. Zheng, J. Balakrishnan, T. Lei, H. R. Kim, Y. I. Song, Y. J. Kim, K. S. Kim, B. Ozyilmaz, J. H. Ahn, B. H. Hong and S. Iijima, *Nat. Nanotechnol.*, 2010, **5**, 574–578.
33 D. R. Dreyer, S. Park, C. W. Bielawski and R. S. Ruoff, *Chem. Soc. Rev.*, 2010, **39**, 228–240.
34 S. Park and R. S. Ruoff, *Nat. Nanotechnol.*, 2009, **4**, 217–224.
35 M. Zhou, Y. L. Wang, Y. M. Zhai, J. F. Zhai, W. Ren, F. A. Wang and S. J. Dong, *Chem.–Eur. J.*, 2009, **15**, 6116–6120.
36 H. Liu, L. Zhang, Y. Guo, C. Cheng, L. Yang, L. Jiang, G. Yu, W. Hu, Y. Liu and D. Zhu, *J. Mater. Chem. C*, 2013, **1**, 3104–3109.
37 W. Gao, L. B. Alemany, L. J. Ci and P. M. Ajayan, *Nat. Chem.*, 2009, **1**, 403–408.
38 E. Kymakis, K. Savva, M. M. Stylianakis, C. Fotakis and E. Stratakis, *Adv. Funct. Mater.*, 2013, **23**, 2742–2749.
39 M. F. El-Kady, V. Strong, S. Dubin and R. B. Kaner, *Science*, 2012, **335**, 1326–1330.
40 Q. Zhuo, Y. Ma, J. Gao, P. Zhang, Y. Xia, Y. Tian, X. Sun, J. Zhong and X. Sun, *Inorg. Chem.*, 2013, **52**, 3141–3147.
41 T. Liu, H. Su, X. Qu, P. Ju, L. Cui and S. Ai, *Sens. Actuators, B*, 2011, **160**, 1255–1261.
42 Q. Bao, D. Zhang and P. Qi, *J. Colloid Interface Sci.*, 2011, **360**, 463–470.
43 W. L. Zhang and H. J. Choi, *Chem. Commun.*, 2011, **47**, 12286–12288.
44 L.-Z. Bai, D.-L. Zhao, Y. Xu, J.-M. Zhang, Y.-L. Gao, L.-Y. Zhao and J.-T. Tang, *Mater. Lett.*, 2012, **68**, 399–401.
45 Q. H. Liu, L. Wei, J. Y. Wang, F. Peng, D. Luo, R. L. Cui, Y. Niu, X. J. Qin, Y. Liu, H. Sun, J. Yang and Y. Li, *Nanoscale*, 2012, **4**, 7084–7089.
46 G. Goncalves, P. A. A. P. Marques, C. M. Granadeiro, H. I. S. Nogueira, M. K. Singh and J. Gracio, *Chem. Mater.*, 2009, **21**, 4796–4802.
47 C. Xu, X. Wang and J. W. Zhu, *J. Phys. Chem. C*, 2008, **112**, 19841–19845.
48 J. Huang, L. M. Zhang, B. A. Chen, N. Ji, F. H. Chen, Y. Zhang and Z. J. Zhang, *Nanoscale*, 2010, **2**, 2733–2738.
49 J. B. Liu, S. H. Fu, B. Yuan, Y. L. Li and Z. X. Deng, *J. Am. Chem. Soc.*, 2010, **132**, 7279–7281.
50 J. Li, D. Kuang, Y. Feng, F. Zhang, Z. Xu, M. Liu and D. Wang, *Biosens. Bioelectron.*, 2013, **42**, 198–206.
51 J. Yang, S. Y. Deng, J. P. Lei, H. X. Ju and S. Gunasekaran, *Biosens. Bioelectron.*, 2011, **29**, 159–166.

52 J. C. Claussen, A. Kumar, D. B. Jaroch, M. H. Khawaja, A. B. Hibbard, D. M. Porterfield and T. S. Fisher, *Adv. Funct. Mater.*, 2012, **22**, 3399–3405.
53 H. T. Yu, P. C. Xu, D. W. Lee and X. X. Li, *J. Mater. Chem. A*, 2013, **1**, 4444–4450.
54 S. Sattayasamitsathit, Y. E. Gu, K. Kaufmann, W. Z. Jia, X. Y. Xiao, M. Rodriguez, S. Minteer, J. Cha, D. B. Burckel, C. M. Wang, R. Polsky and J. Wang, *J. Mater. Chem. A*, 2013, **1**, 1639–1645.
55 S. B. Yang, X. L. Feng, S. Ivanovici and K. Mullen, *Angew. Chem., Int. Ed.*, 2010, **49**, 8408–8411.
56 J. Zhang, Z. P. Zhu, Y. P. Tang and X. L. Feng, *J. Mater. Chem. A*, 2013, **1**, 3752–3756.
57 S. Myung, A. Solanki, C. Kim, J. Park, K. S. Kim and K. B. Lee, *Adv. Mater.*, 2011, **23**, 2221–2225.
58 S. Myung, P. T. Yin, C. Kim, J. Park, A. Solanki, P. I. Reyes, Y. C. Lu, K. S. Kim and K. B. Lee, *Adv. Mater.*, 2012, **24**, 6081–6087.
59 W. G. Xu, J. Q. Xiao, Y. F. Chen, Y. B. Chen, X. Ling and J. Zhang, *Adv. Mater.*, 2013, **25**, 928–933.
60 F. Schwierz, *Nat. Nanotechnol.*, 2010, **5**, 487–496.
61 T. S. Pui, A. Agarwal, F. Ye, N. Balasubramanian and P. Chen, *Small*, 2009, **5**, 208–212.
62 T. S. Pui, A. Agarwal, F. Ye, Y. X. Huang and P. Chen, *Biosens. Bioelectron.*, 2011, **26**, 2746–2750.
63 B. L. Allen, P. D. Kichambare and A. Star, *Adv. Mater.*, 2007, **19**, 1439–1451.
64 K. Lee, P. R. Nair, A. Scott, M. A. Alam and D. B. Janes, *J. Appl. Phys.*, 2009, **105**, 102046.
65 M. S. Makowski and A. Ivanisevic, *Small*, 2011, **7**, 1863–1875.
66 S. Mao, G. Lu, K. Yu, Z. Bo and J. Chen, *Adv. Mater.*, 2010, **22**, 3521–3526.
67 K. Chen, G. Lu, J. Chang, S. Mao, K. Yu, S. Cui and J. Chen, *Anal. Chem.*, 2012, **84**, 4057–4062.
68 C. C. Huang and H. T. Chang, *Anal. Chem.*, 2006, **78**, 8332–8338.
69 T. Zhang, Z. Cheng, Y. Wang, Z. Li, C. Wang, Y. Li and Y. Fang, *Nano Lett.*, 2010, **10**, 4738–4741.
70 H. G. Sudibya, Q. He, H. Zhang and P. Chen, *ACS Nano*, 2011, **5**, 1990–1994.
71 Z. Yin, Q. He, X. Huang, J. Zhang, S. Wu, P. Chen, G. Lu, P. Chen, Q. Zhang, Q. Yan and H. Zhang, *Nanoscale*, 2012, **4**, 293–297.
72 S. Myung, A. Solanki, C. Kim, J. Park, K. S. Kim and K. B. Lee, *Adv. Mater.*, 2011, **23**, 2221–2225.
73 M. E. Melisko, M. Glantz and H. S. Rugo, *Nat. Clin. Pract. Oncol.*, 2009, **6**, 25–33.
74 Y. Y. Shao, J. Wang, H. Wu, J. Liu, I. A. Aksay and Y. H. Lin, *Electroanalysis*, 2010, **22**, 1027–1036.
75 A. Ambrosi and M. Pumera, *Chem.–Eur. J.*, 2010, **16**, 10946–10949.
76 S. Alwarappan, A. Erdem, C. Liu and C.-Z. Li, *J. Phys. Chem. C*, 2009, **113**, 8853–8857.
77 X. Luo, A. Morrin, A. J. Killard and M. R. Smyth, *Electroanalysis*, 2006, **18**, 319–326.
78 Y. Zhuo, R. Yuan, Y. Chai, D. Tang, Y. Zhang, N. Wang, X. Li and Q. Zhu, *Electrochem. Commun.*, 2005, **7**, 355–360.
79 P. A. Fiorito, V. R. Goncales, E. A. Ponzio and S. I. C. de Torresi, *Chem. Commun.*, 2005, 366–368.
80 J.-J. Xu, W. Zhao, X.-L. Luo and H.-Y. Chen, *Chem. Commun.*, 2005, 792–794.
81 L. Gao, W. Yue, S. Tao and L. Fan, *Langmuir*, 2012, **29**, 957–964.
82 Y. Xiao, F. Patolsky, E. Katz, J. F. Hainfeld and I. Willner, *Science*, 2003, **299**, 1877–1881.
83 C. S. Shan, H. F. Yang, D. X. Han, Q. X. Zhang, A. Ivaska and L. Niu, *Biosens. Bioelectron.*, 2010, **25**, 1070–1074.
84 Y. Liu, M. K. Wang, F. Zhao, Z. A. Xu and S. J. Dong, *Biosens. Bioelectron.*, 2005, **21**, 984–988.
85 P. Sorlier, A. Denuziere, C. Viton and A. Domard, *Biomacromolecules*, 2001, **2**, 765–772.
86 C. Shan, H. Yang, J. Song, D. Han, A. Ivaska and L. Niu, *Anal. Chem.*, 2009, **81**, 2378–2382.
87 J. Zhang, K. Sasaki, E. Sutter and R. R. Adzic, *Science*, 2007, **315**, 220–222.
88 S. Zhang, Y. Shao, G. Yin and Y. Lin, *Angew. Chem., Int. Ed.*, 2010, **49**, 2211–2214.
89 E. Katz, I. Willner and J. Wang, *Electroanalysis*, 2004, **16**, 19–44.
90 J. Zhang, J. P. Lei, R. Pan, C. A. Leng, Z. Hu and H. X. Ju, *Chem. Commun.*, 2011, **47**, 668–670.
91 Q. Chen, L. Zhang and G. Chen, *Anal. Chem.*, 2011, **84**, 171–178.
92 W. Qu, L. Zhang and G. Chen, *Biosens. Bioelectron.*, 2013, **42**, 430–433.
93 C. Batchelor-McAuley, Y. Du, G. G. Wildgoose and R. G. Compton, *Sens. Actuators, B*, 2008, **135**, 230–235.
94 X. Cheng, S. Zhang, H. Zhang, Q. Wang, P. He and Y. Fang, *Food Chem.*, 2008, **106**, 830–835.
95 H. C. Chang, X. M. Wang, K. K. Shiu, Y. L. Zhu, J. L. Wang, Q. W. Li, B. A. Chen and H. Jiang, *Biosens. Bioelectron.*, 2013, **41**, 789–794.
96 G. Peng, U. Tisch, O. Adams, M. Hakim, N. Shehada, Y. Y. Broza, S. Billan, R. Abdah-Bortnyak, A. Kuten and H. Haick, *Nat. Nanotechnol.*, 2009, **4**, 669–673.
97 E. A. Jares-Erijman and T. M. Jovin, *Nat. Biotechnol.*, 2003, **21**, 1387–1395.
98 T. Nagai, S. Yamada, T. Tominaga, M. Ichikawa and A. Miyawaki, *Proc. Natl. Acad. Sci. U. S. A.*, 2004, **101**, 10554–10559.
99 H. F. Dong, W. C. Gao, F. Yan, H. X. Ji and H. X. Ju, *Anal. Chem.*, 2010, **82**, 5511–5517.
100 M. Li, X. Zhou, S. Guo and N. Wu, *Biosens. Bioelectron.*, 2013, **43**, 69–74.
101 Y. Tao, Y. H. Lin, Z. Z. Huang, J. S. Ren and X. G. Qu, *Analyst*, 2012, **137**, 2588–2592.
102 X. L. Fu, T. T. Lou, Z. P. Chen, M. Lin, W. W. Feng and L. X. Chen, *ACS Appl. Mater. Interfaces*, 2012, **4**, 1080–1086.

103 X. Ling, L. M. Xie, Y. Fang, H. Xu, H. L. Zhang, J. Kong, M. S. Dresselhaus, J. Zhang and Z. F. Liu, *Nano Lett.*, 2010, **10**, 553–561.
104 W. Ren, Y. Fang and E. Wang, *ACS Nano*, 2011, **5**, 6425–6433.
105 Y. F. Xie, Y. Li, L. Niu, H. Y. Wang, H. Qian and W. R. Yao, *Talanta*, 2012, **100**, 32–37.
106 Y. W. Zhang, S. Liu, L. Wang, X. Y. Qin, J. Q. Tian, W. B. Lu, G. H. Chang and X. P. Sun, *RSC Adv.*, 2012, **2**, 538–545.
107 Y.-T. Li, L.-L. Qu, D.-W. Li, Q.-X. Song, F. Fathi and Y.-T. Long, *Biosens. Bioelectron.*, 2013, **43**, 94–100.
108 M. Liu and W. Chen, *Biosens. Bioelectron.*, 2013, **46**, 68–73.
109 Z. M. Liu, C. F. Hu, S. X. Li, W. Zhang and Z. Y. Guo, *Anal. Chem.*, 2012, **84**, 10338–10344.
110 Z. M. Liu, Z. Y. Guo, H. Q. Zhong, X. C. Qin, M. M. Wan and B. W. Yang, *Phys. Chem. Chem. Phys.*, 2013, **15**, 2961–2966.